JGS
Journal of the Geological Society

Research article

https://doi.org/10.1144/jgs2021-098 | Vol. 179 | 2022 | jgs2021-098

Dating deformation: the role of atomic-scale processes

Igor M. Villa[1,2]

[1] Institut für Geologie, Universität Bern, Baltzerstrasse 3, Bern 3012, Switzerland
[2] Centro Universitario Datazioni e Archeometria, Università di Milano Bicocca, Piazza della Scienza 4, Milano 20126, Italy
IMV, 0000-0002-8070-8142
Correspondence: igor@geo.unibe.ch

Abstract: Dating deformation is difficult, as textures and petrogenesis of deformed rocks are complex. Moreover, geochronometer categories are pursued by communities that often do not communicate.

Hygrochronology dates the retrograde metasomatic/metamorphic reactions caused by aqueous fluid circulation events.

Thermochronology models time-temperature histories by assuming that mineral ages can be uniquely assigned to a 'closure temperature T_c', the only process occurring in rocks being Fick's Law diffusion. Diffusion by definition produces a bell-shaped concentration profile. In contrast, patchy intra-grain isotope concentration profiles denounce aqueous retrogression, whose rate is orders of magnitude faster than diffusion.

Petrochronology is based on opposite assumptions, as the mobility of structure-forming major cations is higher than that of radiogenic Pb, Ar, and Sr. Whenever the formation of a mineral occurs at $T < T_c$, its apparent age dates its formation.

Nanochronology analyses samples at the nanometre-scale. These analyses illuminate atomic-scale processes, e.g. open-system transport of soluble ions along self-sealing networks of nanopores.

The key to dating deformation and producing correct, regional-sized (up to hundreds of kilometres) tectonic models is the realization that minerals consist of atoms, whose behaviour is only firmly constrained by nanometre-scale analyses.

Thematic collection: This article is part of the Isotopic Dating of Deformation collection available at: https://www.lyellcollection.org/cc/isotopic-dating-of-deformation

Received 21 July 2021; **revised** 6 March 2022; **accepted** 7 March 2022

A century ago, Arthur Holmes' (1913) geochronology was still a single discipline, devoted to assigning absolute ages to fossiliferous sedimentary successions, as well as to heretofore undatable 'crystalline' rocks (metamorphic and magmatic). Today it has mutated into a plethora of apparently unrelated subdisciplines, pursued by non-interacting communities. The problem is that the diverging paths followed by the different subdisciplines may end up jeopardizing the credibility of geochronology as a whole, as the predictions and implications provided by geochronology must stand up to independent scrutiny provided by other disciplines of the Earth Sciences. The goal should be instead to restore a context capable of taking into account all facets of the isotopic systems, with the ultimate aim of providing an accurate tool for geological problems whose time-scale ranges from a few ka to several Ga.

The various subdisciplines of geochronology bear names, which highlight one property of the mineral geochronometer that is used by the authors of a study, partly also exploiting different behaviours of the parent-daughter pair(s) that allow the dating of that mineral geochronometer. Thermochronometers (e.g. Malusà and Fitzgerald 2019) are minerals whose age exclusively depends on the temperature, at which the diffusive loss of daughter isotopes (or, in the case of fission tracks, the annealing of the latent tracks with attending resetting of the chronological information) ceased. Their cooling age can be translated to an exhumation rate by assuming a geothermal gradient, constraining a (*P*)-*T*-*t* (pressure – temperature – time) point. Hygrochronometers (Villa and Hanchar 2013) are minerals whose recrystallization, assisted by the circulation of aqueous fluids, dates the episodes of chemical open-system modification of a rock, providing *a*-*X*-*t* (water activity – molar concentration – time) information. If fluid inclusion measurements can constrain the trapping temperature of the fluid, a point in *P*-*T*-*a*-*X*-*t* space can be calculated. Petrochronometers (Kylander-Clark *et al.* 2013) are minerals, on which chemical and isotopic compositions can be simultaneously measured. This enables thermodynamic models (e.g. Holland and Powell 1998; Powell and Holland 2010; Lanari and Duesterhoeft 2019) to relate their chemical composition to the *P*-*T*-*a*-*X* prevailing during their (re) crystallization. Examples are garnet, rutile, titanite, and especially micas (Bosse and Villa 2019). The age given by their isotopic composition yields a point in *P*-*T*-*a*-*X*-*t* space. Nanochronometers (Valley *et al.* 2015) are mineral chronometers (to date, mostly zircon) in which the position of individual atoms is imaged in a three-dimensional map of a few thousand nm^3.

Most prefixes are mutually exclusive. An ideal geochronometer in the sense of Holmes (1913) must be completely retentive of daughter isotopes, otherwise the age of the mineral crystallization is overprinted by later isotope transport processes (be they chemical or thermal, or a combination of both). A hygrochronometer must be a mineral that can be modified by aqueous fluids, and whose retention of radiogenic daughters during chemical modifications was obliterated, as was all other petrological, volcanological and thermal information. A thermochronometer must only record thermally activated, diffusive loss of daughter isotopes, any other temperature-independent process leading to isotope mobility being negligible, as otherwise the inversion of isotope concentrations to infer the ambient temperature is illegitimate. A petrochronometer records metamorphic conditions at the time of its formation without later modifications of the major element composition, and at the same time records its formation age. A nanochronometer can be any of the above, provided it is analysed at the nanometre scale.

One and the same mineral can fulfill contrasting requirements according to the dating method. As an example, apatite can be a thermochronometer when He diffusion is considered (Farley 2002),

a hygrochronometer when hydrothermal circulation is studied (Harlov 2015), and a petrochronometer when it is studied in the context of its paragenesis (Kirkland *et al.* 2018).

For about two thirds of the twentieth century, chronostratigraphy was the most important application of isotopic dating. Dating a 'point-like event' (*sensu* Begemann *et al.* 2001), such as a volcanic eruption and the dispersion of volcanic ash, can be addressed at different scales of accuracy.

If the intended purpose is only the dating of a volcanic sequence, any subsequent fluid circulation events are a nuisance. In submarine and subaerial environments minerals can be weathered, causing systematic age inaccuracy. However, alteration can be turned to advantage, if mineral chronometers are mutated to hygrochronometers (Fuentes *et al.* 2005; cf. also Bosio *et al.* 2020). As mineral alteration is best quantified by electron probe microanalysis (EPMA), it could be argued that the use of petrogenetic/microchemical criteria to support the age assignment of a hygrochronometer falls (strictly speaking) under petrochronology.

The reliability of age assignments can be increased by analysing individual mineral grains (e.g. Bossart *et al.* 1986; Deino and Potts 1992). When calculating the age of a collection of single grain analyses, it is essential to ensure that the analysed grain population is unimodal. A straightforward criterion is the comparison between the external reproducibility of individual grain analyses and the overall standard deviation of the entire population. If the latter is larger than the former, it is highly probable that the population is not unimodal; this is also reflected by the statistical dispersion parameter, MSWD (McIntyre *et al.* 1966), which exceeds the expected value of 1. It must also be pointed out that when MSWD > 1 the probability that the assumed hypothesis (cogeneticity and contemporaneity of the analysed samples) is correct becomes excessively small; in their figure 2, Wendt and Carl (1991) graphically display that this probability becomes 30% if MSWD = 1.1, and drops to 6–20% if MSWD = 1.5. A practical example is taking the average of a collection of values, whereby averaging is only legitimate for a unimodal, random (Gaussian) distribution and illegitimate for a multimodal one. If the dated mineral is monogenetic, the repeat analyses will define a Gaussian distribution. The standard deviation of the latter is expected to be the same as the standard deviation of the repeat analyses of reference materials if the ion beam intensities are the same; this translates to MSWD = 1. If MSWD is high (from 1.6 to 2.5, increasing as the number of degrees of freedom decreases) then the probability that that average be correct is 5%, which obviously means that the contrary hypothesis is 95% likely to be true: the average is meaningless because the distribution is not Gaussian. If this occurs, a systematic bias has exceeded the statistical noise by a factor 19 and it would be a good idea to investigate the cause of this bias so as to remove it. It is a fact that many mineral chronometers are partly retrogressed. Removing devious data points must never be viewed as 'filtering' meant to make the data distribution look Gaussian; what first needs to be understood are the reactions that operated, in order to disentangle primary minerals from secondary retrogression. Whenever a sample is not perfectly unaltered, and its constituent minerals are not strictly monogenetic, the bias is removed by eliminating the petrogenetic outliers (xenocrysts: Deino and Potts 1992; Mana *et al.* 2015; retrograde reaction phases: Glodny *et al.* 2008).

One issue arising when dating metamorphism is that mineral formation could have lasted for a 'long' time. Unlike regional metamorphism, most faults presently exposed have had a 'short' history. Retrogression may well continue after fault movement and deformation have ceased, but the point made here is that peak conditions (forming the main schistosity near the fault plane) are limited to the time duration given by the total displacement divided by the displacement rate.

In the following sections the boundaries between the different flavours of geochronometer minerals will be linked to the geological context, in order to derive the most robust approach for dating deformation.

Thermochronometers

The task of thermochronology is providing numeric inputs for tectonic modelling (including the subsidence history of hydrocarbon-bearing basins). To the extent that the age of a mineral chronometer is exclusively controlled by temperature, it is possible to link the mineral age to the ambient temperature at the time of its isotopic closure. The most widespread thermochronometer is apatite, whose retention of fisson tracks and of radiogenic He occurs around or below 100°C (Farley 2002). To be useful as a thermochronometer, a mineral must have a stability field that does not extend as far down as its 'closure temperature', above which radiogenic daughters are lost from the inert mineral structure. (The concept of the stability field hs two aspects that need to be carefully deistinguished. New growth of a mineral is only allowed in its stability field. Metastable preservation of minerals is allowed even outside the respective stability fields. As an example, garnet does not form at room temperature and pressure, but is metastably preserved in museum collections and jewellers' shops.) If no new mineral can recrystallize, the only process capable of removing radiogenic daughters all while leaving the mineral extant is diffusion. This led Bosse and Villa (2019) to identify this property in their definition of 'Class I' thermochronometers. Fission tracks in apatite are only annealed by temperature, and apatite loses helium only by volume diffusion (sometimes the effective grain size can be reduced by microcracks: Danišík *et al.* 2017). Annealing of fission tracks in, and He loss from, zircon occur at higher temperature and are therefore more prone to additional, albeit mostly subordinate, mechanisms that favour annealing and He loss (Danišík *et al.* 2017; Malusà and Fitzgerald 2019, and references therein).

At even higher temperatures a fundamental problem occurs, which is all too often overlooked for the sake of simplification and convenience. In addition to 'Class I' there exist a very large number of 'Class II' (Bosse and Villa 2019) mineral chronometers, whose lowest stability temperature is lower than their 'closure temperature', above which radiogenic daughters are lost from the inert mineral structure. A Class II mineral that forms much above its 'closure temperature' does not retain radiogenic daughters, so that its age dates the time when it has cooled down to achieve isotopic closure. However, a Class II mineral can also form below its 'closure temperature', in which case its age dates its formation. If its composition can be associated to the *P-T-a-X-d* conditions at the time of its crystallization, a Class II mineral is an efficient petrochronometer (see below).

The empirical determination of 'closure temperatures' is problematic both in the laboratory and in the field. In laboratory experiments it is almost impossible to block diffusion, but other artefacts are possible and even likely, such as superimposing dissolution/reprecipitation onto diffusion. Since the dissolution rate constant, k_{diss}, is orders of magnitude higher than the diffusion rate, D (Villa 2016), it follows that laboratory experiments that are not perfectly anhydrous result in a massive overestimation of the true diffusivity (Hess *et al.* 1987; Villa 2010, 2021). As a result, hydrothermal laboratory experiments give an upper limit for diffusivity but are inadequate to estimate its accurate value.

As a viable alternative to artefact-prone hydrothermal laboratory experiments, the retentivity of a mineral chronometer can be estimated from field relations. If the *P-T-a-X* conditions of a rock are independently known, the preservation or removal of isotopic inheritance in a mineral chronometer constrain its retentivity. An essential note of caution is that the temperature-dependent

retentivity can only be estimated if retrograde reactions were completely absent throughout the rock's history. Unless this is carefully monitored, one can obtain apparently very discrepant field estimates for the same mineral. Examples are monazite (which can retain radiogenic Pb at very high T and lose it at low T – if water promoted retrogression: Seydoux-Guillaume *et al.* 2012), muscovite (which completely retained radiogenic Ar at 560°C but was rejuvenated by fluids below 300°C: Villa *et al.* 2014), biotite (which retained Ar above 500°C: Allaz *et al.* 2011; Airaghi *et al.* 2018, but can be rejuvenated by chloritization in the prehnite-pumpellyite facies), and microcline (which retained Ar at 450°C: Villa and Hanchar 2013, but can be rejuvenated by kaolinitization near room temperature). In summary, empirical retentivity assessments should not take into account an unsupervised average of all field estimates, but only those giving the highest 'closure temperatures', T_c. Lower estimates for T_c usually stem from retrograde reactions, which had not previously investigated using petrological tools to detect major element disequilibrium.

One decisive mathematical argument when examining natural minerals is that Fourier-Fick equations predict that volume diffusion must always result in a bell-shaped concentration gradient (Villa 2016), often referred to as an erf (error function) profile. For multicomponent diffusion in garnet, where charge compensation is involved, Carlson (2017) calculated and observed that REE concentrations deviated from an erf profile. Most studies dealing with concentration gradients in connection with thermochronology address the daughter isotope ^{40}Ar, to which Carlson's (2017) formalism is not applicable. Reported Ar concentration gradients differing from erf profiles contrast with volume diffusion being the process causing isotopic mobility (Phillips and Onstott 1988; Hodges *et al.* 1994). As for the radiogenic Pb isotopes, to this date no Pb concentration profiles with sufficient spatial resolution have been published (cf. Villa 2016). The spatial resolution required for a rigorous identification of a true erf profile is very high (Labotka *et al.* 2004), usually much higher than that achievable with laser microprobes (Villa 2016, fig. 2). The burden of proving the existence of a true erf profile lies on the proponents of the improbable assertion that volume diffusion was the one and only mechanism controlling the isotope record of a mineral chronometer.

If a mineral is entirely enclosed in another mineral, whose diffusivity is extremely low ('armoured inclusion'), the isotopic exchange between the mineral and its surrounding is negligible. In the examples discussed here, and in sheared rocks in general, this armouring did not occur, and the boundary conditions of the diffusion equations do permit isotopic exchange.

The ultimate ground truth test for any theory is whether its predictions are always respected. One single counter-example is sufficient to disqualify a theory as proposed (Popper 1959). Thermochronological modelling applied to micas leads to grossly incorrect tectonic reconstructions (e.g. Steck and Hunziker, as discussed by Bosse and Villa 2019). Observations highlighting the internal inconsistency of thermochronological modelling were discussed, for example, by Balogh and Dunkl (2005) and Airaghi *et al.* (2018). Even past supporters of 'diffusionist' modelling have now come to review the observations and concluded that ages cannot simply be inverted to give a 'cooling history' (e.g. Popov *et al.* 2021). What is observed instead is that some minerals formerly believed to be thermochronometers are in actual fact hygrochronometers, such as K-feldspar (Villa and Hanchar 2013; Chafe *et al.* 2014) and titanite (Holder and Hacker 2019), or petrochronometers, such as monazite (e.g. Villa and Williams 2013), muscovite (Tartèse *et al.* 2011), and biotite (Montemagni *et al.* 2019).

As illustrated in Figure 1c (see the discussion below), if suitable conditions (low water activity and high temperature) prevail, it is possible in principle that diffusion be observable in micas. Indeed, there is one example of biotite in the Oligo-Miocene monometamorphic minerals from the Alps that probably records cooling and not recrystallization, as the rock that contains it is free from retrogression (Allaz *et al.* 2011, fig. 5). There may be another example, a muscovite from the Western Alps, which shows only

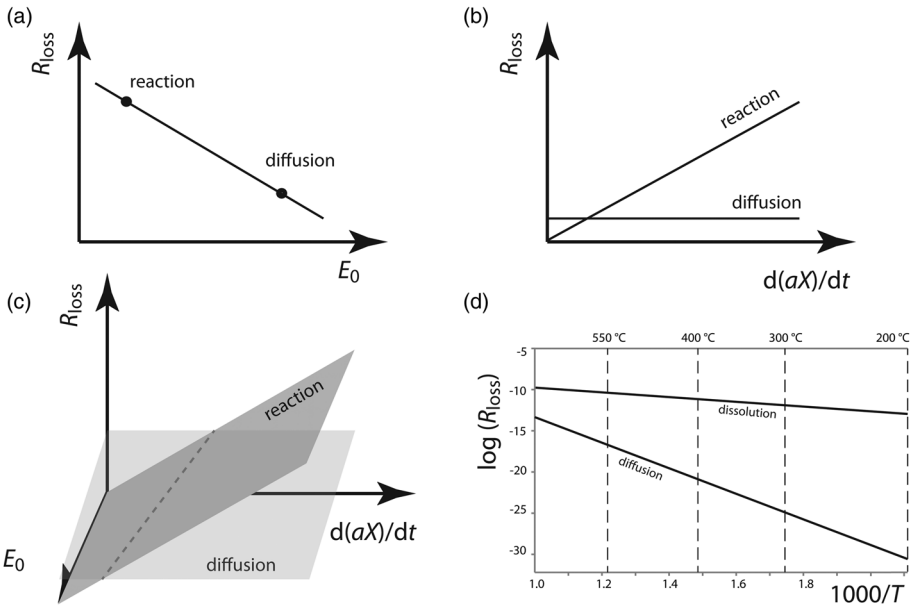

Fig. 1. (**a**) Transport rate of a radiogenic isotope, R_{loss}, v. the energy threshold that an ion of that element must overcome to move in the crystal structure, E_0. Energetically less costly processes have a higher rate unless limited by external factors. (**b**) Transport rate v. the variation in time of reactant availability, d(aX)/dt, at constant temperature. The reactant supply limits or enhances the reaction rate and therefore transport, whereas diffusion always occurs at the same rate for constant boundary conditions. When no reaction occurs, diffusion is the fastest process; as water activity increases, the two processes cross over and reaction effects a faster ion transport than diffusion. (**c**) Combined dependence of R_{loss} on E_0 and d(aX)/dt at constant temperature and boundary condition. The dashed line qualitatively marking the intersection of the two sloping planes separates the regime where diffusion is the fastest process from that where reactions (including dissolution) are faster than diffusion. (**d**) Temperature dependence of the dissolution rate and the diffusion rate for biotite (modified after Villa 2016). The dissolution rate data by Wood and Walther (1983) were obtained between room temperature and 710°C.

limited amounts of chemical variation between its different sieve sizes; this is compatible with only subordinate retrogression (Villa *et al.* 2014, p. 816). Most other micas from the literature record a plurality of isotopic perturbations, from inheritance to alteration.

Hygrochronometers

Hygrochronology did not arise by design from a consciously asked question about hydrogeological systems, but was the unexpected result of mineralogical observations. The first realization that intragrain diachronism could be due to heterochemical retrograde reactions was stimulated by cathodoluminescence (CL) observations of zircon grains (Gebauer *et al.* 1988). Another mineral chronometer that records metasomatic events is monazite. Extensive studies by EPMA of the link between monazite microstructures, their composition, and their age (Williams *et al.* 1999) has established it as a *bona fide* recorder of metasomatism and of fluid circulation events in general (Villa and Williams 2013 and references therein).

Ever since Goldich (1938) the qualitative observation that minerals can and do interact with aqueous fluids can be quantitatively systematized. One of the most labile minerals with respect to aqueous alteration is the feldspar family (cf. also Smith 1974; Smith *et al.* 2013). When attempting to characterize the petrogenesis of an Oligo-Miocene feldspar from the Central Alps, Villa and Hanchar (2013) observed striking variations in its CL emission. This initially surprising analogy to zircon and monazite can be understood by noting that feldspar, much like zircon and monazite, can react with aqueous fluids and recrystallize at virtually any temperature, substantially below its purely temperature-controlled diffusivity (Villa and Hanchar 2013).

Recrystallization occurs in different steps, each of which has independent limiting factors. First, dissolution takes place; its rate depends on water activity a_{H2O}, oxygen fugacity f_{O2}, and temperature T (Wood and Walther 1983). Then, reprecipitation can occur if the solution becomes saturated (by a change in a_{H2O}, and/or f_{O2}, and/or T, and/or a change in the overall fluid composition and the molar fraction X of all cations). Therefore, even if the recrystallization rate R does depend on T, it is not solely dependent on it and the $R(T)$ function cannot be inverted to estimate the ambient T.

The point that the recrystallization rate is not necessarily identical to the dissolution rate is illustrated by the laboratory experiment by Labotka *et al.* (2004). From their figure 2 it can be calculated that the former is lower by almost an order of magnitude than the dissolution rate predicted by Wood and Walther (1983), suggesting that reprecipitation was the slower, rate-limiting process (Villa 2016).

Petrochronometers

Petrochronology endeavours to quantify the 'stratigraphic' sequence of petrogenetic events. One could say that it has come full circle from the goals set by Holmes (1913), by changing the focus on what sequence of geological events one is considering: a century ago, the frontier was dating the sedimentation of a fossiliferous bed; in recent years, the focus has shifted to understanding the passage of a rock through a certain point in *P-T-a-X-d-t* space (*d* being deformation, not truly a petrogenetic indicator *sensu stricto*, but a necessary ingredient to our understanding why a particular chemical reaction came to occur).

The main discriminant between reliable and unreliable petrochronologic inferences is the extent to which it can be unambiguously proved that the *P-T-a-X* information pertains to a thermodynamic equilibrium state that has not been subsequently modified by retrogression reactions or thermally-induced diffusive reequilibration. Even if full re-equilibration is exceptional, it is vital to distinguish between 'mostly equilibrated' and 'vastly retrogressed'. Such disturbances manifest themselves as discrepant *P-T-a-X* estimates (see, e.g. Allaz *et al.* 2011, fig. 5c). Lanari and Duesterhoeft (2019) extended the use of equilibrium thermodynamics to unequilibrated rocks. They noted that even in rocks that were not fully re-equilibrated during metamorphism it was possible to exploit local bulk compositions at the scale of one mineral pair to calculate *P-T-a-X* conditions.

One analytical conundrum in the chemical and isotopic analyses of samples in internal petrologic disequilibrium is the scale of the textures revealing disequilibrium compositions. If the analysed sample volume is excessively large (i.e. larger than natural intragrain heterogeneity), the measurement will smooth away the difference between generations and produce a meaningless 'average' of unrelated subsystems.

Nanochronometers

The possibility to obtain trace element and isotope data with a radically new instrument, the atom-probe (Valley *et al.* 2014), has opened up a new avenue for petrochronological studies. It had long been observed by TEM that below 1 μm, the resolution of the EPMA at the time, there occurred phenomena that were not anticipated in the last century. Especially the formation of clusters of 'parentless Pb' was reported (Seydoux-Guillaume *et al.* 2003; Utsunomiya *et al.* 2004; Kusiak *et al.* 2013). With the possibility to image individual atoms, the transport behaviour of daughter isotopes gains unprecedented clarity (Peterman *et al.* 2019; Seydoux-Guillaume *et al.* 2019). Both radiogenic Pb^{4+} and trace elements such as Y^{3+} do diffuse (as do all atoms at all temperatures above 0 K). The question then became, how far do they diffuse, and why do they form clusters? The length scale travelled by the diffusing ions was a few nanometres, much smaller than the analysed grain size. This means that radiogenic Pb is not 'lost' from a grain but simply redistributed within it: once it has reached an extended defect, where the crystal structure has been damaged by the recoiling α particles, it finds itself in a local potential energy well that ensures its subsequent immobilization. The migration can be enhanced by deformation (Reddy *et al.* 2016).

The formation of clusters of radiogenic daughters trapped in different sites from their radioactive parents thus can give excessively high ages when the resulting heterogeneity is larger than analysed sample volumes. This may seem to prevent geochronologists from obtaining accurate ages at the sub-μm scale. This problem occurs for the opposite reason as the analytical conundrum mentioned above, namely that excessively large sample volumes result in spurious averages. Thus, there appears to be a 'Goldilocks zone' for dating a mineral with a complex microstructure: the analysed volume must be neither larger nor smaller than the microstructures that have previously been characterized. However, the essence of observations of nanometre-sized structures is that geochronologists obtain a direct window for observing the processes at the atomic scale. Fluid flow, with attending chemically open-system transport of soluble ions, was calculated and observed to occur along self-sealing networks of nanopores (Plümper *et al.* 2017). In the absence of pervasive fluid flow, no reequilibration at the μm scale occurs, and chemical and isotopic heterogeneity is preserved.

Atomistic considerations

The assumption that minerals consist of atoms has implications (Lasaga 1981) that have not always been taken into account. Any process involving atoms has a threshold energy, unlike the continuum mechanical approach by Fourier (1822) and Fick (1855). The threshold ('activation energy') that a migrating atom

or ion must overcome in its jump from one unit cell to the next one is inversely proportional to the rate of that process. This is qualitatively illustrated in Figure 1a. The threshold energy for diffusion in phyllosilicates is around 250 kJ mol $^{-1}$ (Villa 2010), that for dissolution 25 kJ mol $^{-1}$ (Smith *et al.* 2013). This alone would ensure that dissolution rates are faster than volume diffuson (Fig. 1d); however, dissolution (as any chemical reaction) is limited by the availability of reactants (Fig. 1b). If enough water is available, the reaction quickly (Wood and Walther 1983) goes to completion and the entire mineral is dissolved. Otherwise, there will remain restitic patches interspersed with dissolved and reprecipitated patches. Combining Figures 1a and b into a three-dimensional plot (Fig. 1c) illustrates the fact that there can exist instances in which fast dissolution is disabled, and slow diffusion remains the predominant process.

Dating deformation: adding '*d*' to *P-T-a-X-t*

If one wants to model the tectonics of a continental mass at the scale of tens or hundreds of kilometres one must first observe the behaviour of minerals at the nanometre scale (Villa 2006). Dating faults is based precisely on the nanometre-scale manifestations of a kilometre-scale stress field. Contrary to older tectonic models of faulting as a purely thermal process affecting petrologically inert rocks (e.g. England and Molnar 1993), faults act, albeit often episodically (Caine *et al.* 1996; Gomila *et al.* 2021), as a preferential conduit for aqueous fluids, with attending mineral recrystallization (Kerrich *et al.* 1980; Proyer 2003). On a fault plane the fluid-induced recrystallization is usually nearly complete and mineral chronometers mostly were reset (Tartèse *et al.* 2012). Near the fault, where relicts of the minerals predating deformation are more abundant, it is essential to perform microchemical and petrological groundwork, without which mass spectrometric measurements are meaningless. The necessity lies in recognizing how many generations of a mineral geochronometer are observable, to what extent each is retrogressed, and which minerals belong together to a single paragenesis. Far from the fault, the earlier mineral generations will be predominant or even exclusive. Similarly, coarser grain sizes will be preferentially more enriched in detrital relicts than the finest grains. In the approach proposed by Árkai *et al.* (1995); cf. Viola *et al.* (2016, 2018), the mixed age obtained from analysing different modal proportion of authigenic and detrital clay generations on a brittle fault plane is plotted as a function of grain size, i.e. of the relicts' proportion. The observed correlation is used to infer the age of the newly crystallized clay component that dates the fault movement.

In higher-grade ductile deformation the authigenic mineral generation dating the deformation phase matures to a grainsize of several tens of μm, very often consisting of a mosaic of intergrown authigenic plus restitic aggregates, and the grain-size approach is much less efficient. However, deconvolving the different generation is still the prerequisite for successful dating. In most deformed rocks, a dedicated microtextural search for heterochemical mineral generations allows a distinction between pre-, syn- and post-deformation minerals. Whenever this petrologic groundwork is not done, analysing random mixtures of diachronous minerals can only yield geologically meaningless average ages. Instead, the identification of microtexturally and compositionally distinct mica generations can be tied to ^{39}Ar-^{40}Ar systematics (as described in detail by Montemagni and Villa 2021) to extract ages for each of them. A failproof discriminant between a Class I thermochronometer and a Class II petrochronometer is provided by the ages of microstructurally different generations of one and the same mineral chronometer (monazite, muscovite, biotite…). If the ages are all different, then at most one of them can be a true cooling age, all lower ages being due to complete (or at least high) retention of radiogenic daughters by mineral generations that (re-)crystallized later than the onset of daughter retention in the oldest generation. If one were to interpret all mica ages as 'cooling ages', inconsistencies become immediately clear (Airaghi *et al.* 2018). If one assumes excessively low retentivity for Ar retention in their biotite (as e.g. their samples from Longmen Shan), and moreover neglects the microstructural observation that biotite-1 predates muscovite-3, then one would be forced to invoke wholesale excess Ar, and all biotite ages would become meaningless; but since biotite gives the same age as allanite, with which it forms contemporaneously, one is forced instead to conclude that biotite retains Ar above 500°C, and that muscovite-3 does not conform to a modelled 'cooling history', since (being a Class II petrochronometer) it records a formation age and not a 'cooling age'. The time-temperature evolution inferred from inaccurate modelling is incorrect and the tectonic reconstruction based on such modelling would be equally incorrect.

In summary, what is required for a reliable dating of deformation is the establishment of a context between microtexture, microchemistry and geochronology. In practical terms, a 'best practice' for dating deformation consists in a well-defined sequence: firstly, microstructurally chart the different textural generations of deformed minerals; then determine the chemical compositions, and their variation, of the observed microstructures; finally, select a dating method that fulfills two essential requirements: allowing a 'Goldilocks' disentanglement of the intergrown mineral generations, and providing control on the effectively achieved disentanglement by the chemical fingerprint (such as, e.g. the ^{208}Pb/^{206}Pb or the ^{38}Ar/^{39}Ar ratios: Villa and Hanchar 2017). All these analyses are labour-intensive, but the reward is a clearer understanding of a superposition of the processes that control the chronological information hidden in deformed rocks.

Acknowledgements Thanks are due to István Dunkl and two unnamed referees for their thoughtful and constructive reviews.

Author contributions **IMV**: conceptualization (lead), data curation (lead), formal analysis (lead), funding acquisition (lead), investigation (lead), methodology (lead), project administration (lead), resources (lead), software (lead), supervision (lead), validation (lead), visualization (lead), writing – original draft (lead), writing – review & editing (lead)

Funding This research received no specific grant from any funding agency in the public, commercial, or not-for-profit sectors.

Competing interests The author declares that he has no known competing financial interests or personal relationships that could have appeared to influence the work reported in this paper.

Data availability Data sharing is not applicable to this article as no datasets were generated or analysed during the current study.

Scientific editing by Christoph von Hagke

References

Airaghi, L., Warren, C.J., de Sigoyer, J., Lanari, P. and Magnin, V. 2018. Influence of dissolution/reprecipitation reactions on metamorphic greenschist to amphibolite facies mica ^{40}Ar/^{39}Ar ages in the Longmen Shan (eastern Tibet). *Journal of Metamorphic Geology*, **36**, 933–958, https://doi.org/10.1111/jmg.12420

Allaz, J., Berger, A., Engi, M. and Villa, I.M. 2011. The effects of retrograde reactions and of diffusion on ^{39}Ar-^{40}Ar ages of micas. *Journal of Petrology*, **52**, 691–716, https://doi.org/10.1093/petrology/egq100

Árkai, P., Balogh, K. and Dunkl, I. 1995. Timing of low-temperature metamorphism and cooling of the Paleozoic and Mesozoic formations of the Bükkium, innermost Western Carpathians, Hungary. *Geologische Rundschau*, **84**, 334–344, https://doi.org/10.1007/s005310050009

Balogh, K. and Dunkl, I. 2005. Argon and fission track dating of Alpine metamorphism and basement exhumation in the Sopron Mts. (Eastern Alps,

Hungary): thermochronology or mineral growth? *Mineralogy and Petrology*, **83**, 191–218, https://doi.org/10.1007/s00710-004-0066-0
Begemann, F., Ludwig, K.R. *et al.* 2001. Call for an improved set of decay constants for geochronological use. *Geochimica et Cosmochimica Acta*, **65**, 111–121, https://doi.org/10.1016/S0016-7037(00)00512-3
Bosio, G., Malinverno, E. *et al.* 2020. Tephrochronology and chronostratigraphy of the Miocene Chilcatay and Pisco formations (East Pisco Basin, Peru). *Newsletters on Stratigraphy*, **53**, 213–247, https://doi.org/10.1127/nos/2019/0525
Bossart, P.J., Meier, M., Oberli, F. and Steiger, R.H. 1986. Morphology versus U-Pb systematics in zircon: a high-resolution isotopic study of a zircon population from a Variscan dike in the Central Alps. *Earth and Planetary Science Letters*, **78**, 339–354, https://doi.org/10.1016/0012-821X(86)90002-6
Bosse, V. and Villa, I.M. 2019. Petrochronology and hygrochronology of tectono-metamorphic events. *Gondwana Research*, **71**, 76–90, https://doi.org/10.1016/j.gr.2018.12.014
Caine, J.S., Evans, J.P. and Forster, C.B. 1996. Fault zone architechture and permeability structure. *Geology*, **24**, 1025–1028, https://doi.org/10.1130/0091-7613(1996)024<1025:FZAAPS>2.3.CO;2
Carlson, W.D. 2017. Multicomponent diffusion in aluminosilicate garnet: coupling effects due to charge compensation. *International Geology Review*, **59**, 526–540, https://doi.org/10.1080/00206814.2016.1189855
Chafe, A.N., Villa, I.M., Hanchar, J.M. and Wirth, R. 2014. A re-examination of petrogenesis and $^{40}Ar/^{39}Ar$ systematics in the the Chain of Ponds K-feldspar: 'diffusion domain' archetype versus polyphase hygrochronology. *Contributions to Mineralogy and Petrology*, **167**, 1010, https://doi.org/10.1007/s00410-014-1010-x
Danišík, M., McInnes, B.I.A., Kirkland, C.L., McDonald, B.J., Evans, N.J. and Becker, T. 2017. Seeing is believing: visualization of He distribution in zircon and implications for thermal history reconstruction on single crystals. *Science Advances*, **3**, 1601121, https://doi.org/10.1126/sciadv.1601121
Deino, A. and Potts, R. 1992. Age-probability spectra for examination of single-crystal $^{40}Ar/^{39}Ar$ dating results: examples from Olorgesailie, southern Kenya rift. *Quaternary International*, **13/14**, 47–53, https://doi.org/10.1016/1040-6182(92)90009-Q
England, P. and Molnar, P. 1993. The interpretation of inverted metamorphic isograds using simple physical calculations. *Tectonics*, **12**, 145–157, https://doi.org/10.1029/92TC00850
Farley, K.A. 2002. (U-Th)/He dating: Techniques, calibrations, and applications. *Reviews in Mineralogy and Geochemistry*, **47**, 819–844, https://doi.org/10.2138/rmg.2002.47.18
Fick, A. 1855. Über Diffusion. *Annalen der Physik*, **94**, 59–86, https://doi.org/10.1002/andp.18551700105
Fourier, J.-B.J. 1822. *Théorie Analytique de la Chaleur*. Didot, Paris.
Fuentes, F., Féraud, G., Aguirre, L. and Morata, D. 2005. $^{40}Ar/^{39}Ar$ dating of volcanism and subsequent very low-grade metamorphism in a subsiding basin: example of the Cretaceous lava series from central Chile. *Chemical Geology*, **214**, 157–177, https://doi.org/10.1016/j.chemgeo.2004.09.001
Gebauer, D., Quadt, A.v., Compston, W., Williams, I.S. and Grünenfelder, M. 1988. Archean zircons in a retrograded Caledonian eclogite of the Gotthard massif (Central Alps, Switzerland). *Schweizerische Mineralogische und Petrographische Mitteilungen*, **68**, 485–490.
Glodny, J., Kuhn, A. and Austrheim, H. 2008. Diffusion versus recrystallization processes in Rb-Sr geochronology: isotopic relics in eclogite facies rocks, Western Gneiss region, Norway. *Geochimica et Cosmochimica Acta*, **72**, 506–525, https://doi.org/10.1016/j.gca.2007.10.021
Goldich, S.S. 1938. A study in rock weathering. *Journal of Geology*, **46**, 17–58, https://doi.org/10.1086/624619
Gomila, R., Fondriest, M. *et al.* 2021. Frictional melting in hydrothermal fluid-rich faults: field and experimental evidence from the Bolfín Fault Zone (Chile). *Geochemistry, Geophysics, Geosystems*, **22**, e2021GC009743, https://doi.org/10.1029/2021GC009743
Harlov, D.L. 2015. Apatite: a fingerprint for metasomatic processes. *Elements*, **11**, 171–176, https://doi.org/10.2113/gselements.11.3.171
Hess, J.C., Lippolt, H.J. and Wirth, R. 1987. Interpretation of $^{40}Ar/^{39}Ar$ spectra of biotites – evidence from hydrothermal degassing experiments and TEM studies. *Chemical Geology*, **66**, 137–149.
Hodges, K.V., Hames, W.E. and Bowring, S.A. 1994. $^{40}Ar/^{39}Ar$ age gradients in micas from a high-temperature-low-pressure metamorphic terrain; evidence for very slow cooling and implications for the interpretation of age spectra. *Geology*, **22**, 55–58, https://doi.org/10.1130/0091-7613(1994)022<0055:AAAGIM>2.3.CO;2
Holder, R.M. and Hacker, B.R. 2019. Fluid-driven resetting of titanite following ultrahigh-temperature metamorphism in southern Madagascar. *Chemical Geology*, **504**, 38–52, https://doi.org/10.1016/j.chemgeo.2018.11.017
Holland, T.J.B. and Powell, R. 1998. An internally consistent thermodynamic data set for phases of petrological interest. *Journal of Metamorphic Geology*, **16**, 309–343, https://doi.org/10.1111/j.1525-1314.1998.00140.x
Holmes, A. 1913. *The Age of the Earth*. Harper & Brothers, London.
Kerrich, R., Allison, I., Barnett, R.L., Moss, S. and Starkey, J. 1980. Microstructural and chemical transformations accom-panying deformation of granite in a shear zone at Mieville, Switzerland. *Contributions to Mineralogy and Petrology*, **73**, 221–242, https://doi.org/10.1007/BF00381442
Kirkland, C.L., Yakymchuk, C., Szilas, K., Evans, N., Hollis, J., McDonald, B. and Gardiner, N.J. 2018. Apatite: a U-Pb thermochronometer or geochronometer? *Lithos*, **318–319**, 143–157, https://doi.org/10.1016/j.lithos.2018.08.007
Kusiak, M.A., Whitehouse, M.J., Wilde, S.A., Nemchin, A.A. and Clark, C. 2013. Mobilization of radiogenic Pb in zircon revealed by ion imaging: implications for early Earth geochronology. *Geology*, **41**, 291–294, https://doi.org/10.1130/G33920.1
Kylander-Clark, A.R.C., Hacker, B.R. and Cottle, J.M. 2013. Laser-ablation split-stream ICP petrochronology. *Chemical Geology*, **345**, 99–112 https://doi.org/10.1016/j.chemgeo.2013.02.019
Labotka, T.C., Cole, D.R., Fayek, M., Riciputi, L.R. and Stadermann, F.J. 2004. Coupled cation and oxygen-isotope exchange between alkali feldspar and aqueous chloride solution. *American Mineralogist*, **89**, 1822–1825, https://doi.org/10.2138/am-2004-11-1229
Lanari, P. and Duesterhoeft, E. 2019. Modeling metamorphic rocks using equilibrium thermodynamics and internally consistent databases: past achievements, problems and perspectives. *Journal of Petrology*, **60**, 19–56, https://doi.org/10.1093/petrology/egy105
Lasaga, A.C. 1981. The atomistic basis of kinetics: defects in minerals. *Reviews in Mineralogy*, **8**, 261–319.
Malusà, M.G. and Fitzgerald, P.G. (eds) 2019. *Fission-track Thermochronology and its Application to Geology*. Springer, Heidelberg.
Mana, S., Furman, T., Turrin, B.D., Feigenson, M.D. and Swisher, C.C., III 2015. Magmatic activity across the East African North Tanzanian Divergence Zone. *Journal of the Geological Society, London*, **172**, 368–389, https://doi.org/10.1144/jgs2014-072
McIntyre, G.A., Brooks, C., Compston, W. and Turek, A. 1966. The statistical assessment of Rb-Sr isochrons. *Journal of Geophysical Research*, **71**, 5459–5468, https://doi.org/10.1029/JZ071i022p05459
Montemagni, C. and Villa, I.M. 2021. Geochronology of Himalayan shear zones: unravelling the timing of thrusting from structurally complex fault rocks. *Journal of the Geological Society, London*, **178**, jgs2020-235, https://doi.org/10.1144/jgs2020-235
Montemagni, C., Montomoli, C., Iaccarino, S., Carosi, R., Jain, A.K., Massonne, H.-J. and Villa, I.M. 2019. Dating protracted fault activity: microstructures, microchemistry and geochronology of the Vaikrita thrust, Main Central Thrust zone, Garhwal Himalaya, NW India. *Geological Society, London, Special Publications*, **481**, 127–146, https://doi.org/10.1144/SP481.3
Peterman, E.M., Reddy, S.M., Saxey, D.W., Fougerouse, D., Snoeyenbos, D.R. and Rickard, W.D.A. 2019. Nanoscale processes of trace element mobility in metamorphosed zircon. *Contributions to Mineralogy and Petrology*, **174**, 92, https://doi.org/10.1007/s00410-019-1631-1
Phillips, D. and Onstott, T.C. 1988. Argon isotopic zoning in mantle phlogopite. *Geology*, **16**, 542–546, https://doi.org/10.1130/0091-7613(1988)016<0542:AIZIMP>2.3.CO;2
Plümper, O., Botan, A., Los, C., Liu, Y., Malthe-Sørenssen, A. and Jamtveit, B. 2017. Fluid-driven metamorphism of the continental crust governed by nanoscale fluid flow. *Nature Geoscience*, **10**, 685–690, https://doi.org/10.1038/ngeo3009
Popov, D.V. *et al.* 2021. Multi-method approach to understanding the migration mechanisms of Pb in apatite and Ar in alkali feldspar from Proterozoic granitic batholiths from the Mt. Isa Inlier (Australia). Virtual Goldschmidt Abstract, 21–6981.
Popper, K. 1959. *The Logic of Scientific Discovery*. Hutchinson, London.
Powell, R. and Holland, T.J.B. 2010. Using equilibrium thermodynamics to understand metamorphism and metamorphic rocks. *Elements*, **6**, 309–314, https://doi.org/10.2113/gselements.6.5.309
Proyer, A. 2003. The preservation of high-pressure rocks during exhumation: metagranites and metapelites. *Lithos*, **70**, 183–194, https://doi.org/10.1016/S0024-4937(03)00098-7
Reddy, S.M., van Riessen, A. *et al.* 2016. Mechanisms of deformation-induced trace element migration in zircon resolved by atom probe and correlative microscopy. *Geochimica et Cosmochimica Acta*, **195**, 158–170, https://doi.org/10.1016/j.gca.2016.09.019
Seydoux-Guillaume, A.-M., Goncalves, P., Wirth, R. and Deutsch, A. 2003. Transmission electron microscope study of polyphase and discordant monazites: site-specific specimen preparation using the focused ion beam technique. *Geology*, **31**, 973–976, https://doi.org/10.1130/G19582.1
Seydoux-Guillaume, A.-M., Montel, J.M. *et al.* 2012. Low-temperature alteration of monazite: fluid mediated coupled dissolution–precipitation, irradiation damage, and disturbance of the U–Pb and Th–Pb chronometers. *Chemical Geology*, **330–331**, 140–158, https://doi.org/10.1016/j.chemgeo.2012.07.031
Seydoux-Guillaume, A.-M., Fougerouse, D., Laurent, A., Gardés, E., Reddy, S. and Saxey, D. 2019. Nanoscale resetting of the Th/Pb system in an isotopically-closed monazite grain: a combined atom probe and transmission electron microscopy study. *Geoscience Frontiers*, **10**, 65–76, https://doi.org/10.1016/j.gsf.2018.09.004
Smith, J.V. 1974. *Feldspar Minerals*, **2**. Springer, Heidelberg.
Smith, M.M., Wolery, T.J. and Carroll, S.A. 2013. Kinetics of chlorite dissolution at elevated temperatures and CO_2 conditions. *Chemical Geology*, **347**, 1–8, https://doi.org/10.1016/j.chemgeo.2013.02.017
Tartèse, R., Ruffet, G., Poujol, M., Boulvais, P. and Ireland, T.R. 2011. Simultaneous resetting of the muscovite K-Ar and monazite U-Pb geochronometers: a story of fluids. *Terra Nova*, **23**, 390–398, https://doi.org/10.1111/j.1365-3121.2011.01024.x
Tartèse, R., Boulvais, P., Poujol, M., Chevalier, T., Paquette, J.L., Ireland, T.R. and Deloule, E. 2012. Mylonites of the South Armorican Shear Zone: insights

for crustal-scale fluid flow and water-rock interaction processes. *Journal of Geodynamics*, **56–57**, 86–107, https://doi.org/10.1016/j.jog.2011.05.003

Utsunomiya, S., Palenik, C.S., Valley, J.W., Cavosie, A.J., Wilde, S.A. and Ewing, R.C. 2004. Nanoscale occurrence of Pb in an Archean zircon. *Geochimica et Cosmochimica Acta*, **68**, 4679–4686, https://doi.org/10.1016/j.gca.2004.04.018

Valley, J.W., Cavosie, A.J. *et al.* 2014. Hadean age for a post-magma-ocean zircon confirmed by atom-probe tomography. *Nature Geoscience*, **7**, 219–223, https://doi.org/10.1038/ngeo2075

Valley, J.W., Reinhard, D.A. *et al.* 2015. Nano-and micro-geochronology in Hadean and Archean zircons by atom-probe tomography and SIMS: new tools for old minerals. *American Mineralogist*, **100**, 1355–1377, https://doi.org/10.2138/am-2015-5134

Villa, I.M. 2006. From the nm to the Mm: isotopes, atomic-scale processes, and continent-scale tectonic models. *Lithos*, **87**, 155–173, https://doi.org/10.1016/j.lithos.2005.06.012

Villa, I.M. 2010. Disequilibrium textures vs equilibrium modelling: geochronology at the crossroads. *Geological Society, London, Special Publications*, **332**, 1–15, https://doi.org/10.1144/SP332.1

Villa, I.M. 2016. Diffusion in mineral geochronometers: present and absent. *Chemical Geology*, **420**, 1–10, https://doi.org/10.1016/j.chemgeo.2015.11.001

Villa, I.M. 2021. The *in vacuo* release of Ar from minerals: 1. hydrous minerals. *Chemical Geology*, **564**, 120076, https://doi.org/10.1016/j.chemgeo.2021.120076

Villa, I.M. and Hanchar J.M. 2013. K-feldspar hygrochronology. *Geochimica et Cosmochimica Acta*, **101**, 24–33, https://doi.org/10.1016/j.gca.2012.09.047

Villa, I.M. and Hanchar J.M. 2017. Age discordance and mineralogy. *American Mineralogist*, **102**, 2422–2439, https://doi.org/10.2138/am-2017-6084

Villa, I.M. and Williams, M.L. 2013. Geochronology of metasomatic events. *In*: Harlov, D.E. and Austrheim, H. (eds) *Metasomatism and the Chemical Transformation of Rock*. Springer, Heidelberg, 171–202.

Villa, I.M., Bucher, S., Bousquet, R., Kleinhanns, I.C. and Schmid, S.M. 2014. Dating polygenetic metamorphic assemblages along a transect through the Western Alps. *Journal of Petrology*, **55**, 803–830, https://doi.org/10.1093/petrology/egu007

Viola, G., Scheiber, T., Fredin, O., Zwingmann, H., Margreth, A. and Knies, J. 2016. Deconvoluting complex structural histories archived in brittle fault zones. *Nature Communications*, **7**, 13448, https://doi.org/10.1038/ncomms13448

Viola, G., Torgersen, E., Mazzarini, F., Musumeci, G., van der Lelij, R., Schönenberger, J. and Garofalo, P.S. 2018. New constraints on the evolution of the inner northern apennines by K-Ar dating of late miocene-early pliocene compression on the island of Elba, Italy. *Tectonics*, **37**, 3229–3243, https://doi.org/10.1029/2018TC005182

Wendt, I. and Carl, C. 1991. The statistical distribution of the mean squared weighted deviation. *Chemical Geology*, **86**, 275–285, https://doi.org/10.1016/0168-9622(91)90010-T

Williams, M.L., Jercinovic, M.J. and Terry, M.P. 1999. Age mapping and dating of monazite on the electron microprobe: deconvoluting multistage tectonic histories. *Geology*, **27**, 1023–1026, https://doi.org/10.1130/0091-7613(1999)027<1023:AMADOM>2.3.CO;2

Wood, B.J. and Walther, J.V. 1983. Rates of hydrothermal reactions. *Science*, **222**, 413–415, https://doi.org/10.1126/science.222.4622.413